similar to those for linearly interacting systems, there are notable differences that depend on the strength of the quadratic-interaction parameter. These are the shape and resolution of the zero-phonon line; the temperature dependence and, to a lesser extent, the shape of the broad band; the occurrence of mirror symmetry of the low-temperature absorption and emission spectra; and the relation of the high-temperature absorption and emission spectra. From the temperature dependence of the shape of broad band and the observation of zero-phonon lines, values of the linear- and quadratic-interaction parameters can be estimated from experimental spectra.

ACKNOWLEDGMENT

The author is appreciative for the computer program drawn up by T. W. Crimmins for computation of the line intensities.

[1]F. E. Williams, J. Chem. Phys. 19, 457 (1951).
[2]F. E. Williams and M. H. Hebb, Phys. Rev. 84, 1181 (1951).
[3]F. E. Williams, Phys. Rev. 82, 281 (1951).
[4]M. Lax, J. Chem. Phys. 20, 1752 (1952).
[5]J. T. Ritter, J. Chem. Phys. 53, 3461 (1970).
[6]J. T. Ritter and J. J. Markham, Phys. Rev. 185, 1201 (1969).
[7]J. J. Markham, Rev. Mod. Phys. 31, 956 (1959).
[8]T. H. Keil, Phys. Rev. 140, A601 (1965).
[9]T. H. Keil and A. Gold, Phys. Rev. 140, A906 (1965).
[10]C. S. Kelley and F. E. Williams (unpublished).
[11]M. Mostoller, B. N. Ganguly, and R. F. Wood, Phys. Rev. B 4, 2015 (1971).
[12]J. B. Coon, R. E. DeWames, and C. M. Loyd, J. Mol. Spectroscopy 8, 285 (1962).
[13]C. S. Kelley, Edgewood Arsenal Technical Report No. 4575, 1971 (unpublished).

PHYSICAL REVIEW B VOLUME 6, NUMBER 11 1 DECEMBER 1972

Relaxation of Local-Moment Nuclei in Metals

R. E. Walstedt
Bell Laboratories, Murray Hill, New Jersey 07974
and
A. Narath
Sandia Laboratories, Albuquerque, New Mexico 87115
(Received 27 April 1972)

Relaxation processes for the nuclei of dilute S-like local moments in metals are investigated using both perturbation and dynamic-susceptibility techniques. In contrast to host nuclear relaxation, terms analogous to the Benoit–de Gennes–Silhouette (BGS) and Giovannin–Heeger (GH) processes are obtained in the local case by working only to second order in J_{sd}. The two methods of calculation are found, using the dynamic susceptibilities of Götze and Wölfle, to agree exactly within the approximations used. Contrary to the traditional view, the BGS process is found to consist of both real and virtual local-moment-excitation terms, becoming a purely *virtual* mechanism for large H_0/T. The GH process appears as an interference effect between the first-order (Korringa) term and the virtual BGS term. A similar relationship is believed to hold in the host-relaxation case. The local T_2 is found to behave rather differently from T_1 at low temperatures, with T_1 and T_2 merging into a single isotropic field-independent rate for sufficiently small H_0/T. The present calculations provide a qualitative understanding of the AgMn:^{55}Mn saturation results given by Okuda and Date.

I. INTRODUCTION

The relaxation of bulk metal nuclei by relatively dilute local moments has by now been studied quite extensively, both in terms of theory[1–4] and experiment.[5–8] In this paper we investigate the related question of relaxation processes for the local-moment nuclei themselves in such systems, e.g., of the ^{55}Mn nuclei in dilute CuMn or AgMn. It will be seen that such nuclear relaxation processes can be very rapid. Our first objective in calculating their strength is to determine under what conditions one might hope to apply the powerful methods of pulsed NMR to the observation of these resonances.

The motivation for such experiments is similar to that for the host-relaxation measurements, namely, to study the fluctuation properties of dilute moments in metals. On this basis the local-moment nuclear relaxation has the advantages of (a) being, in general, much larger than the background Korringa rate and (b) avoiding the difficult questions of host-hyperfine-coupling strength, spatial averages of relaxation-rate contributions,

and wipeout or diffusion-barrier radii.

In addition to the above points, the present work is also motivated by some valuable insights it provides into the nature of host-relaxation processes.[1,3,4] Because the hyperfine coupling with the local-moment nucleus is given *a priori* and does not have to be generated by the perturbation terms, we find in second-order time-dependent perturbation theory, the analogs of the Benoit–de Gennes–Silhouette[1] (BGS) and Giovannini–Heeger[3] (GH) processes. These processes are often said[4,6,8] to involve real and virtual excitations of the impurity moment, respectively. Our calculations show that this distinction is an artificial one. The BGS process is found to consist of both real and virtual excitations of the impurity moment, and, in fact, to be given only by purely *virtual* excitations for large H/T.

The longitudinal relaxation process is calculated with both perturbation and dynamic-susceptibility techniques. Using the dynamic susceptibilities calculated recently by Götze and Wölfle[9] we find exact agreement between the two results.

We also apply the dynamic-susceptibility technique to the calculation of the transverse relaxation time T_2. Because this process samples a different part of the local-moment fluctuation spectrum and because these fluctuations are anisotropic for large H/T, T_2 and T_1 behave in a drastically different fashion. We shall see that T_2 will usually be the deciding factor in determining the observability of the resonance by transient methods.

There do not appear to be quantitative data in the literature on the relaxation rates calculated here. In Sec. IV we make a rough comparison with the AgMn : ^{55}Mn saturation results of Okuda and Date.[10] In the final section the implications of this work for host-relaxation processes are summarized.

II. PERTURBATION THEORY OF T_1

Our initial approach is to analyze the relaxation processes for the nucleus of an isolated local moment which occur in first- and second-order perturbation theory. The conduction-electron–local-moment interaction is described by the usual s-d exchange model. The question of interaction effects at finite concentrations is touched on briefly in Sec. IV. No bottleneck effects are anticipated here; however, no analysis of this question is attempted.

The unperturbed Hamiltonian is taken to be

$$\mathcal{H}_0 = \sum_{\vec{k},\sigma} \epsilon_{\vec{k},\sigma} c^\dagger_{\vec{k},\sigma} c_{\vec{k}\sigma} - h_d S^z - h_n I^z \,, \tag{1}$$

where the $\epsilon_{\vec{k},\sigma} = \epsilon_{\vec{k}} - h_s\sigma$ are the energies of noninteracting conduction electrons of spin σ. S^z and I^z are z components of spin operators for the local atomic and nuclear moments, respectively. $h_{d,s} = g_{d,s}\mu_B H_0$ and $h_n = \gamma H_0$ are the various Zeeman splittings, and we note that h_d and h_s are negative. We take $\hbar = 1$ throughout. Consideration is restricted to S-like local moments.[11]

For the coupling between $\vec{I}$, $\vec{S}$ and conduction-electron-spin operator $\vec{s}$, we take

$$\mathcal{H}' = \sum_{\vec{k},\sigma,\vec{k}',\sigma'} J_{\vec{k}',\vec{k}} c^\dagger_{\vec{k}\sigma} [S^z s^z_{\sigma\sigma'} + \tfrac{1}{2}(S^+ s^-_{\sigma\sigma'} + S^- s^+_{\sigma\sigma'})] c_{\vec{k}'\sigma'}$$
$$+ \sum_{\vec{k},\sigma,\vec{k}',\sigma'} A_{\vec{k}',\vec{k}} c^\dagger_{\vec{k}\sigma} [I^z s^z_{\sigma\sigma'} + \tfrac{1}{2}(I^+ s^-_{\sigma\sigma'} + I^- s^+_{\sigma\sigma'})] c_{\vec{k}'\sigma'}$$
$$+ A_d \vec{I}\cdot\vec{S} \,, \tag{2}$$

where the first two terms represent the s-d exchange and Fermi contact interactions, respectively, the last being the core-polarization hyperfine coupling associated with d and f moments. Note that $\vec{s} = \frac{1}{2}(\hat{i}\sigma_x + \hat{j}\sigma_y + \hat{k}\sigma_z)$, where the $\sigma_{x,y,z}$ are Pauli matrices.

There are myriad effects contained in the total Hamiltonian (1) plus (2), such as the electron-spin-resonance (ESR) linewidths, Kondo condensation, etc. Here we assume Kondo phenomena are unimportant and focus only on nuclear relaxation processes; as we shall see, the results have implications for the ESR linewidths as well. Considering T_1 first, we evaluate those processes which change the nuclear-spin quantum number from m to $m+1$. In addition to the usual Korringa[12] process, we see from Eq. (2) that three types of processes occur in second order, namely, those involving $J_{\vec{k}',\vec{k}}$ and s-electron hyperfine coupling, $J_{\vec{k}',\vec{k}}$ and d-electron hyperfine coupling, and those which are quadratic in the hyperfine coupling. The last of these contributions is extremely small and will henceforth be neglected.

For the cross terms involving $J_{\vec{k}',\vec{k}}$ and one of the hyperfine operators, there are four nonvanishing second-order processes giving $\Delta m = 1$. In Table I, states for these processes are listed in terms of the four quantum numbers m, m_s, $\vec{k}$, and σ which characterize the eigenstates of the un-

TABLE I. Table of intermediate states for second-order nuclear-spin transitions in which the system quantum state goes from $n = (m,\ m_s,\ \vec{k},\ \sigma)$ to either $n' = (m+1,\ m_s,\ \vec{k}',\ \sigma-1)$ [(a) and (c)] or to $n' = (m+1,\ m_s-1,\ \vec{k}',\ \sigma)$ [(b) and (d)]. Transitions are labeled with hyperfine couplings which drive them.

(Conduction-electron spin)		(Local-moment spin)	
(a) $\Delta m_s = 0$	(b) $\Delta m_s = -1$	(c) $\Delta m_s = 0$	(d) $\Delta m_s = -1$
$m+1/m$	$m+1/m$	$m+1/m$	$m+1/m$
m_s/m_s	m_s/m_s-1	m_s-1/m_s+1	m_s-1/m_s
$\sigma-1/\sigma$	$\sigma-1/\sigma+1$	$\sigma/\sigma-1$	σ/σ
$\vec{k}''/\vec{k}''$	$\vec{k}''/\vec{k}''$	$\vec{k}/\vec{k}$	$\vec{k}/\vec{k}'$

perturbed Hamiltonian (1). Both possible intermediate states are listed for each process. It will be noted that a process with $\Delta m_s = -2$, $\Delta\sigma = 1$ is also allowed by these perturbation terms. However, the second-order matrix element for that vanishes, and thus the tabulated list is complete.

The transition rate for $m \to m+1$ is given by

$$W_{m+1,m}^{(\Delta m_s)} = 2\pi \sum_{m_s} P(m_s) \times \sum_{\vec{k}',\sigma',\vec{k},\sigma} f(\vec{k},\sigma)[1 - f(\vec{k}',\sigma')] \left| M_{n'n}^{(\Delta m_s)} \right|^2 \delta(\epsilon' - \epsilon) , \quad (3)$$

where $P(m_s)$ is the occupation probability of state m_s, f is the Fermi occupation function, and $M_{n'n}^{(\Delta m_s)}$ is the total matrix element for transitions from initial state n to final state n' (see Table I). The second-order portion of $M_{n'n}^{(\Delta m_s)}$ is given by

$$\sum_{n''} \frac{\langle n' | \mathcal{H}' | n'' \rangle \langle n'' | \mathcal{H}' | n \rangle}{\epsilon - \epsilon''} , \quad (4)$$

where the sum is over all possible intermediate states n''. At this point we note a major difference between the conduction-electron and local-moment hyperfine processes, namely, that for the former there is a continuum of intermediate-state energies (due to $\epsilon_{\vec{k}''}$), because neither perturbation is diagonal in $\vec{k}$. It is shown in the Appendix that this leads to an essential cancellation of most of the second-order matrix element, leading to results of the order of J/E_F times the first-order matrix element (E_F is the Fermi energy). For this reason we omit any further discussion of these terms.

In calculating rates we note that process (c) of Table I interferes with the Korringa process, thus we add the first-order matrix element $\frac{1}{2}\langle m+1 \times |I^+| m \rangle A_{\vec{k}',\vec{k}}$ to that of (c). Further, in order to continue the calculation, we assume $NA_{\vec{k}',\vec{k}} = \text{const} = A_s$ and replace $NJ_{\vec{k}',\vec{k}}$ with a suitable average value J_{sd}, where N is the number of atoms in the system. A_s and J_{sd} then correspond to wave functions normalized in one atomic volume. For the two processes which remain under consideration, Eq. (3) gives

$$W_{m+1,m}^{(0)} = \tfrac{1}{2}\pi(I-m)(I+m+1)\, h_n (1 - e^{-\beta h_n})^{-1} n^2(E_F) \times \sum_{m_s} P(m_s)[A_s + m_s A_d J_{sd} / (h_n - h_d)]^2 \quad (5)$$

and

$$W_{m+1,m}^{(-1)} = \frac{\tfrac{1}{4}\pi(I-m)(I+m+1)\, A_d^2 J_{sd}^2 n^2(E_F) \sum_{m_s} P(m_s)[S(S+1) - m_s^2 + m_s]}{(h_n - h_d)(1 - e^{-\beta(h_n - h_d)})} \quad (6)$$

in the spherical-band approximation with $n(E_F)$ the density of states for one spin direction in cgs units/atom and $\beta = (kT)^{-1}$. Equations (5) and (6) give the major second-order contributions to nuclear relaxation. The terms in J_{sd}^2 can be seen to be of the order of $J_{sd}^2/(h_n - h_d)^2$ times the first-order rate; for moderate field values this will in some instances constitute a multiplication factor of several orders of magnitude. We note that the inverse rates to (5) and (6) are easily shown to satisfy thermodynamic detailed-balance conditions when $P(m_s)$ is a thermal-equilibrium distribution.

With Eq. (5) we can identify three distinct T_1 contributions, namely, the first-order (Korringa) rate $\propto A_s^2$, the second-order (so) contribution $\propto J_{sd}^2$, and a cross term $\propto A_s A_d J_{sd}$. In the (usual) limit $\beta h_n \ll 1$ the cross-relaxation contribution becomes

$$1/T_1(\text{cross}) = 2\pi k T n^2(E_F) A_s A_d J_{sd} \langle S^z \rangle / (h_n - h_d). \quad (7)$$

This is seen to be the local-moment analog of the GH process[3] for host nuclei. Both $1/T_1(\text{cross})$ and the GH process involve virtual excitation of the impurity moment ($\Delta m_s = 0$). Furthermore, if we identify A_d with the transferred hyperfine coupling to a host nucleus $\propto A_s J_{sd}$, then the analogy concerning dependence on A_s, J_{sd}, T, and H_0 is complete. We note also that such a cross term, as in the case of the GH term, is not necessarily positive.

Combining the second-order part of (5) with (6) we find in the further approximation $|h_n / h_d| \ll 1$, the total second-order rate contribution

$$\frac{1}{T_1(\text{so})} = \frac{\pi k T A_d^2 J_{sd}^2 n^2(E_F)}{h_d^2} \left(S(S+1) - \langle S^z \rangle \coth(\beta h_d / 2) + \frac{\langle S^z \rangle h_d \beta}{2[\cosh(\beta h_d) - 1]} \right) . \quad (8)$$

In discussing Eq. (8), it must be remarked that there are several ranges in the value of the quantity H_0/T which must be distinguished. First, we note that the whole second-order perturbation treatment is only valid in the limit $|h_d T_2^e| \gg 1$, where $1/T_2^e$ is the width of the local-moment ESR line. With $1/T_2^e = \pi J_{sd}^2 n^2(E_F) kT$,[13] this condition becomes

$$h_d \beta \gg \pi J_{sd}^2 n^2(E_F) , \quad (9)$$

where the right-hand side is generally much less than unity. Only in this limit is m_s a good quantum number. For smaller values of $h_d\beta$ we shall see in Sec. III that T_1(so) has a different functional form.

Further, in Eq. (8) the quantity in large parentheses changes its value in the neighborhood of $h_d\beta \sim 1$, approaching $\frac{2}{3}S(S+1)$ for $h_d\beta \ll 1$ and S^2 for $h_d\beta \gg 1$. Apart from this transition region, then, within condition (9) $1/T_1(\mathrm{so})$ varies basically as T/H_0^2.

We note two further points of interest concerning $T_1(\mathrm{so})$ as given by Eq. (8). First, this relaxation process is generated entirely by local-moment fluctuations and second, it results from a combination of real [$\Delta m_s = \pm 1$, Eq. (6)] and virtual [$\Delta m_s = 0$, Eq. (5)] local-moment excitations. The two types of excitation make equal-rate contributions at high temperatures; at low temperatures $1/T_1(\mathrm{so})$ is generated *entirely by virtual excitations*.

III. DYNAMIC-SUSCEPTIBILITY APPROACH

A. Longitudinal Relaxation

It is of interest to derive $1/T_1(\mathrm{so})$ by means of the dynamic-susceptibility formalism to see that both methods give essentially the same result. More importantly, this scheme will make it clear that $1/T_1(\mathrm{so})$ is the precise analog of the BGS mechanism for host nuclear relaxation. It is frequently stated that the BGS process results from real excitation of the impurity moment.[4,6,8] The present work shows, however, that real excitations are only partially involved at high temperatures and that BGS relaxation at low temperatures is generated entirely by virtual spin flips.

To proceed with our derivation, the longitudinal relaxation rate due to coupling with a spin $\vec{s}$ is given by[14]

$$1/T_1 = \tfrac{1}{2}A_d^2 \int_{-\infty}^{\infty} [\langle S_x S_x(\tau)\rangle + \langle S_y S_y(\tau)\rangle] e^{-i\omega_n \tau} d\tau, \tag{10}$$

where the angular brackets denote a thermodynamic average. By the fluctuation-dissipation theorem, Eq. (10) may be rewritten

$$\frac{1}{T_1} = \frac{A_d^2}{g^2\mu_B^2(1-e^{-\omega_n\beta})} \operatorname{Im}[\chi_{xx}(\omega_n) + \chi_{yy}(\omega_n)], \tag{11}$$

where χ_{xx} and χ_{yy} are components of the local-moment dynamic-susceptibility tensor. We take both of these quantities to be equal to the transverse local-moment susceptibility derived by Götze and Wölfle;

$$\operatorname{Im}\chi_T(\omega) = \omega N''(\omega)\{(\omega - h')^2 + [N''(\omega)/\chi_T^0]^2\}^{-1}, \tag{12}$$

with

$$N''(\omega) = \tfrac{1}{4}\pi[g\mu_B J_{sd} n(E_F)]^2\{2\langle S^{z2}\rangle + \omega^{-1}\langle S^z\rangle(\omega - h') \times[\coth(\tfrac{1}{2}\beta(\omega - h')) + \coth(\tfrac{1}{2}\beta h')]\}, \tag{13}$$

where h' is the local-moment spin-resonance frequency including possible conduction-electron-shift effects, and $\chi_0^T = g\mu_B\langle S^z\rangle/H_0$. With $N''(\omega)$ evaluated at $\omega = h'$, (12) and (13) give the spin-resonance line shape, correctly modified for relaxation to the instantaneous field,[15] with $1/T_2^e = N''(h')/\chi_T^0$. The resulting linewidth expression coincides with that given by Orbach and Spencer[16] when specialized to their case of an effective spin $S = \frac{1}{2}$.

For the present application we identify h' with h_d from Sec. II and take $N''(\omega) \cong N''(0) = \chi_T^0/T_2^e(0)$. $1/T_2^e(0)$ is the effective spin-resonance linewidth at zero frequency and differs slightly from $1/T_2^e$. With $\omega_n\beta \ll 1$, Eq. (11) then becomes

$$\frac{1}{T_1(\mathrm{so})} = \frac{2A_d^2 kT\chi_0^T}{g^2\mu_B^2 T_2^e(0)}\left[(h_n - h_d)^2 + \left(\frac{1}{T_2^e(0)}\right)^2\right]^{-1}. \tag{14}$$

In the perturbation limit (9), (14) becomes (neglecting h_n)

$$\frac{1}{T_1(\mathrm{so})} \cong \frac{\pi A_d^2 kTJ_{sd}^2 n^2(E_F)}{h_d^2}\left(S(S+1) - \langle S^z\rangle\coth(\beta h_d/2) + \frac{\langle S^z\rangle h_d\beta}{2[\cosh(\beta h_d) - 1]}\right). \tag{15}$$

Equation (15) is seen to be the same as the perturbation expression (8).

It is useful to point out a detailed physical connection between corresponding terms in Eqs. (8) and (15). The first two (large parentheses) terms in (8) arise from the $\Delta m_s = 0$ transition rate (5), whereas in (15) they can be traced to the $\Delta m_s = \pm 1$ contribution to $1/T_2^e$.[9] On the other hand, the final term in (8) is given by the $\Delta m_s = \pm 1$ transition rate (6), and the corresponding term in (15) can be seen to arise from the z-axis ($\Delta m_s = 0$) fluctuation part of $1/T_2^e$.[9]

This criss-crossed correspondence, surprising at first, turns out to be just what one expects if the second-order T_1 process is viewed as two successive steps. In each case we may consider a mutual nuclear-atomic spin flip to be one step, changing m_s by one unit. To obtain $\Delta m_s = 0$ over all, this is accompanied by a cancelling atomic flip with the conduction electrons. The latter process gives the $\Delta m_s = \pm 1$ thermodynamic character to the virtual transition (5). Likewise, in the real ($\Delta m_s = \pm 1$) process (6), the nuclear flip must be accompanied by a $\Delta m_s = 0$ conduction-electron scattering process. It is gratifying that two rather different approaches to the problem, i.e., here and in Ref. 9 yield the same result. In this sense, Eq. (8) can be said to corroborate the susceptibility (12) given by Götze and Wölfle.[9]

The connection between $1/T_1(\mathrm{so})$ and the BGS T_1 mechanism for host nuclei is apparent from Eq. (11). There, if we replace A_d with a transferred-hyperfine-coupling coefficient $A_s \operatorname{Re}\chi^e(R_j, \omega_n)$, the same expression results as identified in Ref. 4 as the BGS relaxation rate. Here $\chi^e(R_j, \omega_n)$ is the

conduction-electron transfer susceptibility. It is obvious that the BGS rate expression could also be derived by the perturbation technique, leading to the conclusion stated earlier regarding the importance of virtual processes.

In the case of moment nuclei studied here, we see that the BGS and GH relaxation processes are very intimately connected. This is especially true at low temperatures, with both processes as well as the Korringa rate given by Eq. (5) alone.

B. Transverse Relaxation

It is necessary to make a separate investigation of the local-moment nuclear T_2 process, both because the fluctuations are highly anisotropic at low temperature and because T_1 and T_2 sample different parts of the frequency spectrum. The total transverse relaxation rate is given by[14]

$$1/T_2 = 1/(2T_1) + \tfrac{1}{2}A_d^2\left[\int_{-\infty}^{\infty}\langle S_z S_z(\tau)\rangle e^{-i\omega\tau}d\tau\right]_{\omega\to 0}, \tag{16}$$

where we shall refer to the z-axis fluctuation term as $1/T_{2z}$. Again we use the fluctuation-dissipation theorem to relate $1/T_{2z}$ to the dynamic longitudinal susceptibility, taking the latter quantity from the work of Götze and Wölfle,[9] $\chi^L(\omega) = \chi_0^L/(1 - i\omega T_1^e)$, where $\chi_0^L = g\mu_B \partial\langle S^z\rangle/\partial H_0$. The result is

$$1/T_{2z} = \frac{A_d^2 k T T_1^e}{g\mu_B}\,\frac{\partial\langle S^z\rangle}{\partial H_0}, \tag{17}$$

with

$$1/T_1^e = \frac{\pi g^2\mu_B^2 J_{sd}^2 n^2(E_F)\beta h_d\langle S^z\rangle}{4\sinh^2(\beta h_d/2)\chi_0^L}.$$

Evaluating (17) at high temperatures, we find $1/T_{2z}$ proportional to T^{-1} and field independent. At low temperatures T_1^e approaches a constant value and $\partial\langle S^z\rangle/\partial H_0$ vanishes exponentially. For arbitrary field and temperature, (17) becomes

$$\frac{1}{T_{2z}} = \frac{4A_d^2\sinh^2(\beta h_d/2)\{(S+\frac{1}{2})^2\operatorname{csch}^2[(S+\frac{1}{2})\beta h_d] - \frac{1}{4}\operatorname{csch}^2(\beta h_d/2)\}^2}{\pi h_d J_{sd}^2 n^2(E_F)\{(S+\frac{1}{2})\coth[(S+\frac{1}{2})\beta h_d] - \frac{1}{2}\coth(\beta h_d/2)\}}. \tag{18}$$

T_{2z} senses the fluctuation density at zero frequency and, therefore, in contrast with T_1 as given by (15), goes *inversely* as the square of J_{sd}.

At sufficiently high temperatures and low fields, i.e., the opposite limit from condition (9), the local-moment linewidth becomes large compared with all Zeeman splittings. It follows that the nuclear relaxation must be isotropic and field independent in this limit. That this is so may be seen from Eq. (14), which, with $h_d T_2^e \ll 1$ and the high-temperature correspondences $\chi_0^L = \chi_0^T$ and $T_1^e = T_2^e$, becomes twice T_{2z}^{-1} [Eq. (17)]. Equation (16) then gives $T_2 = T_1$ as required.

IV. APPLICATIONS

By way of illustration, calculated values of $1/T_1$(so) [Eq. (8)] and $1/T_{2z}$ [Eq. (18)] are plotted in Figs. 1 and 2, respectively, for the case of dilute *Cu*Mn, where we take $A_d = 44\times10^{-4}$ cm^{-1},[17] $g = 2$, $J_{sd}\sim 1$ eV,[18] and $n(E_F) = 0.16$ eV^{-1}atom^{-1}. The calculations have been carried out for a range of likely experimental values of H_0 and T. For the parameters given, the cross term [Eq. (7)] is negligible throughout. It is assumed that the Mn-impurity moment is characterized by $S = \frac{5}{2}$. For this spin value the asymptotic $\beta h_d \ll 1$ and $\beta h_d \gg 1$ values in the large parentheses in Eq. (8) are 5.83 and 6.25, respectively, yielding a nearly temperature-independent coefficient of T/H_0^2 in the plot of T_1^{-1}. The dashed lines show the deviation of T_1^{-1} at low fields and high temperatures [Eq. (14)] from the simple perturbation result.

In assessing the transverse relaxation rates one must bear in mind that half the rates in Fig. 1 must be added to $1/T_{2z}$ to give the total rate [Eq. (16)]. Although there is some uncertainty about the true value of J_{sd} for this case, it is clear from the plotted results that the region of experimental interest for spin-echo technique is (a) limited to low temperatures and high fields, specifically to $H_0 > 40$ kG and $T < 2\,^\circ$K for the case shown; and (b) determined primarily by T_{2z} and therefore more constricted for smaller values of J_{sd}.

For alloys with a finite concentration there will obviously be important modifications to the relaxation rates calculated here due to Ruderman–Kittel–Yosida (RKY) exchange couplings among the impurities.[7] In the limit of a dense ferromagnet $1/T_1$(so) goes over to the mechanism discussed by Weger,[19] which is severely limited by requirements of ferromagnon $\vec{k}$ conservation.

Very little experimental data is available on the relaxation rates calculated here. One possible application is to the case of ~1-at.% Mn in Cu or Ag at helium temperature studied by Okuda and Date[10] using an electron-nuclear-double-tensor (ENDOR) technique. It was found that the ESR line of the Mn in *Ag*Mn could be caused to shift slightly by saturating the ^{55}Mn polarization with rf power. In this way the ^{55}Mn NMR line was located at ~250 MHz, in good agreement with the nuclear-orientation work of Cameron *et al.*[17]

The precise conditions of saturation are not discussed in Ref. 10; however, we may make a crude estimate of T_1 from the coil geometry and power level stated. Assuming the absence of any kind of

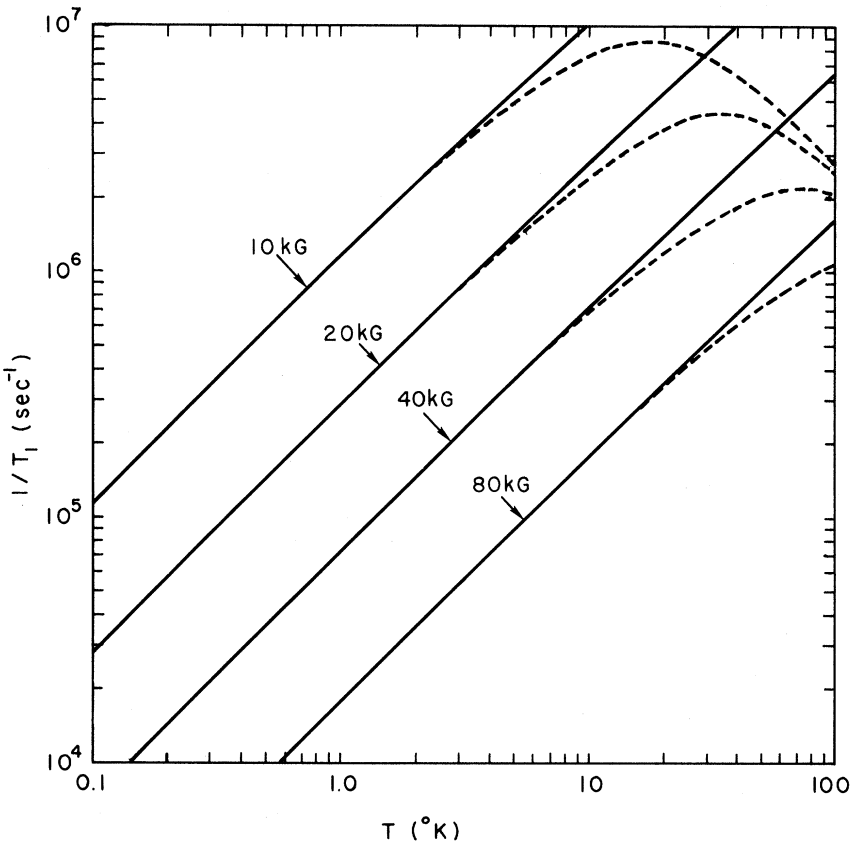

FIG. 1. Second-order longitudinal relaxation rate for a local-moment nucleus plotted against temperature for several applied field values, using hyperfine, exchange, and local-moment parameters given in the text. The transition region for $g\mu_B H_0 \sim kT$ is very nearly invisible for $S = \frac{5}{2}$. Dashed lines show approach to field-independent $T_1 \propto T$ at high temperatures.

resonator (none is mentioned), we find $\gamma H_1 \sim 1/T_1 \sim 10^3$ sec^{-1}. This is faster by a factor $\sim 10^3$ than a typical s-electron relaxation process, confirming at least that a strong contribution from local-moment fluctuations is present.

Although we cannot make a quantitative correspondence with the single-impurity calculations of this paper, comparison of the above T_1 estimate with Fig. 1 suggests that at $T = 1\,^\circ$K the large RKY exchange couplings are severely inhibiting the second-order T_1 process. Regarding the magnetic states in these alloys as essentially local in character,[20] RKY couplings may be viewed in a molecular-field picture to correspond roughly to $H_0 \sim T_c/k \sim 10^5$ G, where T_c is the "ordering" temperature. With this assumption, and noting further a possible rf enhancement of ~ 2, we find consistency with the T_1 estimate to within an order of magnitude.

V. SUMMARY AND DISCUSSION

A perturbation calculation of relaxation processes for local-moment nuclei yields a BGS-like[1] term in second order and a GH-like[3] term as a cross term between the BGS and Korringa[12] matrix elements. The similarity to the original GH [3] term is inevitable because of nearly identical starting Hamiltonians. Contrary to the traditional view, the BGS-like term consists of both local-moment spin-flip and non-spin-flip (real and virtual) processes, a conclusion which presumably applies to relaxation of host nuclei as well. For $g\mu_B H_0/kT \gg 1$, the real process "freezes" out, and all nuclear relaxation takes place through virtual excitations of the local moment.

The above picture is corroborated by a dynamic-susceptibility calculation of the second-order relaxation. In the (high-field) region where the two calculations are comparable, the real and virtual terms in $1/T_1$(so) are found to correspond, interestingly, with $\Delta m_s = \pm 1$ terms in the local-moment dynamic susceptibility,[9] respectively. This is easily understood in terms of a two-step process, with $\Delta m_s = \pm 1$ in the first step to flip to nucleus; the contributing dynamic-susceptibility term is characterized by whatever *additional* change in m_s is brought about in a concomitant conduction-electron scattering process. Thus, the low-temperature virtual excitations of the previous paragraph (such as the GH process) behave thermodynamically like spin-flip conduction-electron scattering.

Viewed another way, the perturbation and dynamic susceptibility treatments of the nuclear T_1 pro-

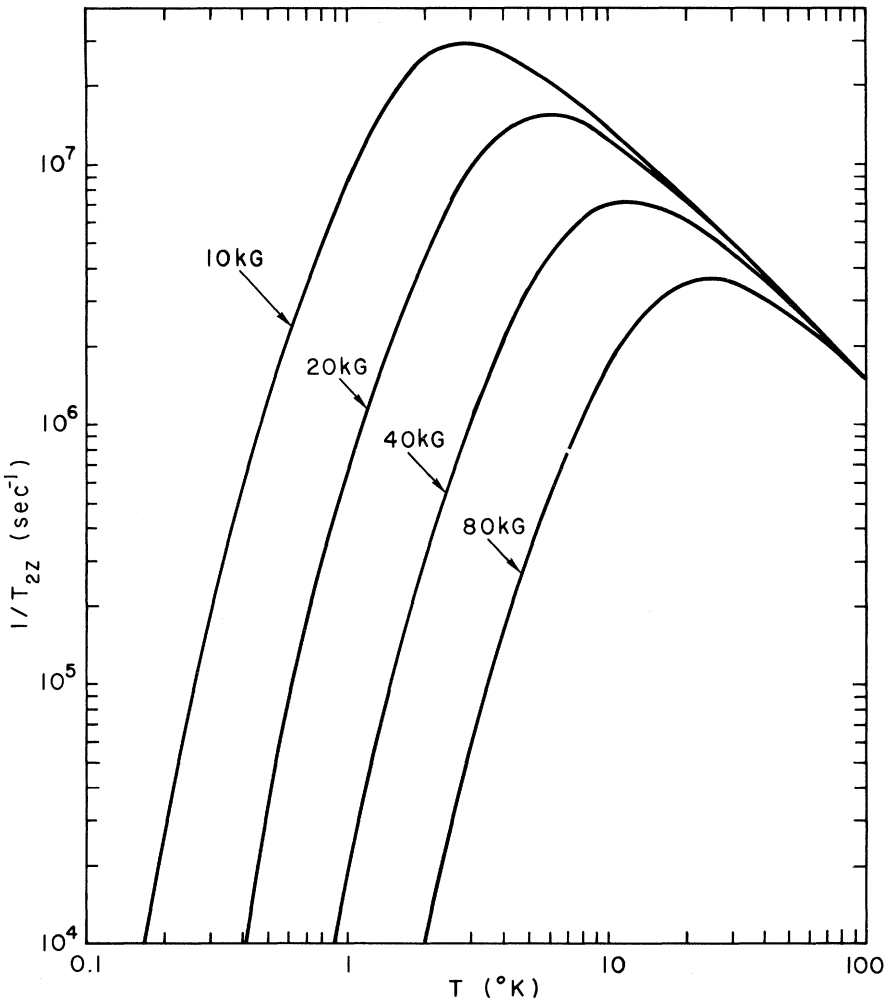

FIG. 2. Contribution to transverse relaxation rate from z-axis local-moment fluctuations ($1/T_{2z}$) plotted against temperature for several applied field values, using parameters given in the text.

cess may be combined to check the local-moment ESR linewidth given by Götze and Wölfle.[9] It is especially interesting that the frequency dependence of this quantity [Eq. (13)] is corroborated by the perturbation calculation.

The present treatment demonstrates in a fundamental way the evidently close connection between the local GH and BGS relaxation processes. This is thought to be the case for host nuclei as well, as can be seen, for example, by extending the GH[3] analysis to next-higher order. The development of Sec. II is essentially equivalent to such an extension.

Finally, our results suggest that the direct observation of ^{55}Mn NMR in *Cu*Mn and *Ag*Mn, as well as other systems, should be feasible at sufficiently high fields and low temperatures. In the ENDOR work of Okuda and Date,[10] it is suggested that the large internal RKY fields allowed the ^{55}Mn NMR in $Ag\mathrm{Mn}_{0.01}$ to be saturated at modest power levels. Work is currently underway to observe the ^{55}Mn NMR directly in these systems.

ACKNOWLEDGMENT

The authors wish to thank Dr. P. Wölfle for valuable suggestions concerning the use of his susceptibility results (Ref. 9).

APPENDIX

To illustrate our point concerning the second-order matrix elements of conduction-electron hyperfine processes in Table I, we consider process (a) explicitly:

$$M_{n'n}^{(0)} = \tfrac{1}{4} m_s \langle m+1 | I^+ | m \rangle \times \sum_{\vec{k}''} \left(\frac{A_{\vec{k}'\vec{k}''} J_{\vec{k}''\vec{k}}}{\epsilon_{\vec{k}} - \epsilon_{\vec{k}''}} - \frac{J_{\vec{k}'\vec{k}''} A_{\vec{k}''\vec{k}}}{\epsilon_{\vec{k}'} - \epsilon_{\vec{k}''}} \right) . \quad \text{(A1)}$$

On converting the sum on $\vec{k}''$ to an integral, the first term in large parentheses becomes

$$\tfrac{1}{4} m_s \langle m+1 | I^+ | m \rangle \times \int \frac{d\epsilon}{\epsilon_{\vec{k}} - \epsilon} \int_{\epsilon} \frac{1}{(2\pi)^3} \frac{dS_{k''}}{|\vec{\nabla}_{k''} \epsilon|} A_{\vec{k}'\vec{k}''} J_{\vec{k}''\vec{k}} , \quad \text{(A2)}$$

where the $\int_{\epsilon} dS_{\vec{k}}$ is taken over the surface of constant energy ϵ in $\vec{k}''$ space and is of order $n(\epsilon)A_s J_{sd}$. We denote this integral $U(\vec{k}', \vec{k}, \epsilon)$ and assume it to be a a well-behaved function of ϵ for $\vec{k}$ and $\vec{k}'$ values of interest. In performing $\int d\epsilon$ in (A2), it is shown by Schiff[21] that the path of integration should pass under singularities on the real axis. The final result for the first term in (A1) then becomes

$$\tfrac{1}{4} m_s \langle m+1 | I^+ | m \rangle \left(\left\{ \mathcal{P} \int \frac{U(\vec{k}', \vec{k}, \epsilon)\, d\epsilon}{(\epsilon_{\vec{k}} - \epsilon)} + i\pi U(\vec{k}', \vec{k}, \epsilon_{\vec{k}}) \right\} \right) . \quad \text{(A3)}$$

Barring irregular behavior of U, the quantity in large parentheses in (A3) is of order $A_s J_{sd}/\epsilon_F$ as was to be shown.

The above argument can be carried through in a similar fashion for process (b) of Table I as well, leading to the conclusion that terms (a) and (b) both produce relatively small corrections to the Korringa process.

[1] H. Benoit, P. G. de Gennes, and D. Silhouette, Compt. Rend. 256, 3841 (1963).

[2] R. Orbach and P. Pincus, Compt. Rend. 257, 1271 (1963).

[3] B. Giovannini and A. J. Heeger, Solid State Commun. 7, 287 (1969).

[4] B. Giovannini, P. Pincus, G. Gladstone, and A. J. Heeger, J. Phys. (Paris) 32, C1-163 (1971).

[5] O. J. Lumpkin, Phys. Rev. 164, 324 (1967).

[6] P. Bernier, H. Launois, and H. Alloul, J. Phys. (Paris) 32, C1-513 (1971).

[7] M. R. McHenry, B. G. Silbernagel, and J. H. Wernick, Phys. Rev. Letters 27, 426 (1971).

[8] F. Y. Fradin, Phys. Rev. Letters 26, 1033 (1971).

[9] W. Götze and P. Wölfle, J. Low Temp. Phys. 5, 575 (1971).

[10] K. Okuda and M. Date, J. Phys. Soc. Japan 27, 839 (1969).

[11] Non-S-state moments are excluded from the present treatment because both their relaxation properties and hyperfine couplings are expected to be quite different from those considered here.

[12] J. Korringa, Physica 16, 601 (1950).

[13] H. Hasegawa, Progr. Theoret. Phys. (Kyoto) 21, 483 (1959).

[14] A. Abragam, *The Principles of Nuclear Magnetism* (Oxford U. P., Oxford, England, 1961), p. 310.

[15] Ref. 10, Chap. III.

[16] R. Orbach and H. J. Spencer, Phys. Letters 26A, 457 (1968).

[17] J. A. Cameron, I. A. Campbell, J. P. Compton, R. A. G. Lines, and G. V. H. Wilson, Phys. Letters 20, 569 (1966).

[18] R. E. Behringer, J. Phys. Chem. Solids 2, 209 (1957).

[19] M. Weger, Phys. Rev. 128, 1505 (1962).

[20] P. W. Anderson, Mater. Res. Bull. 5, 549 (1970).

[21] L. I. Schiff, *Quantum Mechanics* (McGraw-Hill, New York, 1955), Chap. VIII.

PHYSICAL REVIEW B VOLUME 6, NUMBER 11 1 DECEMBER 1972

Further EPR Studies of Forbidden Hyperfine Transitions of Mn^{2+} in Calcite*

V. Lupei† and A. Lupei†

Argonne National Laboratory, Argonne, Illinois 60439

and

I. Ursu

Institute for Atomic Physics, Bucharest, Romania

(Received 18 February 1972)

A study of the forbidden hyperfine transitions up to $\Delta m = \pm 5$ within the central fine-structure component of the EPR spectrum of Mn^{2+} in calcite is reported. The line positions are interpreted with spin-Hamiltonian parameters previously determined and with a quadrupole-interaction parameter of 0.5 ± 0.1 G. Two approaches were used for calculating line intensities; perturbation theory and the effective-electron–magnetic field method. Good agreement with experiment was obtained.

INTRODUCTION

Forbidden hyperfine transitions ($\Delta M = \pm 1$, $\Delta m \neq 0$) have been observed in the electron-paramagnetic-resonance (EPR) spectra of Mn^{2+} in a series of crystals. The great majority of these investigations have dealt with $\Delta M = \pm 1$, $\Delta m = \pm 1$ transitions, while transitions of larger values of Δm have seldom been considered. Important requirements for the occurrence of forbidden transitions in the spectrum of the $Mn^{2+}(^6S)$ ion are that (i) the fine-structure parameter be large enough, and (ii) the lines